Localization and fluctuations in quantum kicked rotors

Indubala I. Satija*
Department of Physics, George Mason University, Fairfax, Virginia 22030

Bala Sundaram†
Department of Mathematics, 1S215 CSI-CUNY, 2800, Victory Boulevard, Staten Island, New York 10314

Jukka A. Ketoja
KCL Paper Science Centre, P.O. Box 70, FIN-02151 Espoo, Finland
(Received 18 February 1999)

We address the issue of fluctuations, about an exponential line shape, in a pair of one-dimensional kicked quantum systems exhibiting dynamical localization. An exact renormalization scheme establishes the fractal character of the fluctuations and provides a method to compute the localization length in terms of the fluctuations. In the case of a linear rotor, the fluctuations are independent of the kicking parameter k and exhibit self-similarity for certain values of the quasienergy. For given k, the asymptotic localization length is a good characteristic of the localized line shapes for all quasienergies. This is in stark contrast to the quadratic rotor, where the fluctuations depend upon the strength of the kicking and exhibit local ''resonances.'' These resonances result in strong deviations of the localization length from the asymptotic value. The consequences are particularly pronounced when considering the time evolution of a packet made up of several quasienergy states. [S1063-651X(99)09807-4]

PACS number(s): 05.45.−a, 03.65.Sq, 75.30.Kz, 64.60.Ak

Dynamical localization is an important manifestation of the quantum suppression of diffusive classical motion resulting from nonintegrable dynamics [1–5]. As the name suggests, the mechanism is analogous to the Anderson description of a low-dimensional, low-temperature insulator phase in terms of tight-binding models (TBM) [6,7]. The relationship between these two seemingly disparate systems was made explicit [3] in a class of kicked quantum Hamiltonians of the form (in dimensionless units)

$$H=K(p)+V(\theta)\sum \delta(t-n), \tag{1}$$

where $K(p)$ denotes a general kinetic energy operator. Note that time is measured in units of spacing between kicks. The time-periodic nature of the Hamiltonian allows the time-dependent solution to be expressed, in terms of the one-step evolution operator U, as

$$U\psi(\theta,t)=\psi(\theta,t+1). \tag{2}$$

For kicked systems, U takes on the particularly simple form

$$U=\exp[-iK(p)/\hbar]\exp[-iV(\theta)/\hbar], \tag{3}$$

where $\hbar$ refers to the effective quantization scale in dimensionless units. Further, the evolution of any initial condition can be expressed in terms of quasienergy states ϕ_ω which satisfy

$$U\phi_\omega=e^{-i\omega}\phi_\omega, \tag{4}$$

where the quasienergy ω is real as U is a unitary operator.

The relationship between these quantum kicked systems and TBM becomes clear on projecting the quasienergy states onto eigenstates of $K(p)$. In our context, these are angular momentum states. The equation satisfied by the projection coefficients u_m onto the mth angular momentum state is [3]

$$T_m u_m+\sum_r W_{m-r}u_r=0, \tag{5}$$

where

$$T_m=\tan\{[\omega-K(m)]/2\}, \tag{6}$$

and the W_m are the Fourier weights of

$$W(\theta)=-\tan[V(\theta)/2\hbar], \tag{7}$$

with respect to the angular momentum basis. This transformation provides a simple method to understand dynamical localization and recurrences in energy in kicked rotors.

In this mapping, the integer angular momentum quantum number of the rotor corresponds to the lattice site in TBM. The free phase evolution between kicks provides the pseudorandom diagonal (on-site) potential while the kicking potential $V(\theta)$ determines the range and strength of the hopping. Thus, under certain conditions, boundedness and recurrences in energy in the kicked rotor manifest themselves in quasienergy states which are exponentially localized on a lattice labeled by the angular momentum quantum number m of the rotor.

From a practical standpoint, this method of studying kicked rotors is particularly useful when the TBM contains only nearest-neighbor couplings. This has motivated many

*Electronic address: isatija@sitar.gmu.edu
†Electronic address: bas@math.csi.cuny.edu

 ©1999 The American Physical Society

studies [3,8] of a special class of kicked rotors where the potential is chosen to be $V(\theta) = -2\hbar \arctan[k\cos(\theta)]$, resulting in a TBM,

$$T_m u_m + \frac{k}{2}(u_{m+1} + u_{m-1}) = 0. \tag{8}$$

Note that we, unlike earlier treatments, explicitly retain the presence of the quantization scale $\hbar$ in the definition of the potential. This makes it clear why the classical limits of quantum rotors corresponding to this choice of potential are trivial. The TBM, however, are perfectly well defined and serve as useful illustrative examples.

This nearest-neighbor TBM has been studied [3] for linear and quadratic rotors which are described by $K(p) = \sigma p$, where σ is an irrational number, and $K(p) = p^2/2$. In the diagonal term in the TBM, these translate into $K(m) = \sigma m$ and $K(m) = \hbar m^2/2$, respectively. Thus, $\hbar$ does not explicitly appear in the TBM analysis of the linear rotor. In the quadratic rotor we set $\hbar = 8\pi\sigma$ in keeping with the requirements of dynamical localization [5].

The linear rotor, where the diagonal disorder is quasiperiodic, was solved exactly. In particular, the density of states was shown to be identical to the average density of states for the Lloyd model of disorder [8] for which the T_m are independent random variables with the Cauchy distribution

$$P(T_m) = \frac{1}{\pi}\frac{1}{1+T_m^2}. \tag{9}$$

Furthermore, the numerically computed localization length was found to be in good agreement with the analytic, ensemble averaged, inverse localization length $\bar{\gamma}$ of the Lloyd model [8],

$$\cosh(\bar{\gamma}) = \sqrt{k^{-2}+1}. \tag{10}$$

The localization length γ^{-1} depends upon k and controls the transient and recurrence time scales in the system. For the quadratic rotor where the diagonal disorder is pseudorandom, statistical studies of the sequences T_m showed similarities with the random potential with Lorentzian distribution. It was argued that in spite of some correlations, the quadratic model also exhibits the localization characteristics of the Lloyd model [3,4]. However, our work here shows that *these residual correlations have a profound impact on the fluctuations in the line shape*. These, in turn, can lead to strong deviations of γ^{-1} from the ideal Lloyd model prediction.

In this paper, we directly compute the fluctuations in the exponential line shape for linear and quadratic rotors. We compare and contrast the linear, integrable, system with equally spaced quasienergies, $\omega_j = j\sigma \bmod(1)$ (independent of k) and the quadratic, nonintegrable case, where the quasienergies depend upon k. We reiterate that the classical limit of the Lloyd model is not well defined, and so integrability or not refers only to the distribution of the energy levels. In other words, *the terminology merely distinguishes between the two cases we consider and does not imply a classical limit*.

Our motivation is to understand better how the two different $K(p)$ in the kicked rotor are manifested in the localization properties of the equivalent TBMs. We characterize the differences in these two rotor systems by using a recent technique [9] for studying the fluctuations in the respective localized quasienergy states. We begin by factoring out the exponential envelope. Thus the projections of the eigenstates of the rotor u_m are written as

$$u_m = e^{-\bar{\gamma}|m|}\eta_m, \tag{11}$$

where η_m are the fluctuations in the localized states at the mth lattice site. Thus, the fluctuations η_m can be related to the fluctuations in the localization length γ (where $u_m = e^{-\gamma}$) as

$$\gamma - \bar{\gamma} = -\ln|\eta_m|/m. \tag{12}$$

As explained below, we use an exact decimation scheme to compute the scaling properties of the fluctuations η_m thereby establishing the fact that these are fractal. Furthermore, the scale length γ^{-1} need not be presupposed but can be self-consistently determined. It should be noted that this equation is valid for any TBM including random systems. Therefore, the method described above can be used to compute localization length for any nearest-neighbor TBM irrespective of the nature of diagonal or off-diagonal disorder.

The fluctuations η_m satisfy the following TBM:

$$e^{-\bar{\gamma}}\eta_{m+1} + e^{\bar{\gamma}}\eta_{m-1} + \lambda T_m \eta_m = 0, \tag{13}$$

where $\lambda = 2/k$. We apply a recently developed decimation method [9] to this TBM. σ in T_m was taken to be the inverse golden mean $(\sqrt{5}-1)/2$. In this approach, the incommensurability of the lattice was exploited by decimating all sites except those labeled by the Fibonacci numbers F_n. This renormalization group approach was shown to be an extremely useful tool to demonstrate self-similarity and to obtain universal characteristics of quasiperiodic systems. Here, we apply this formalism to a linear rotor, described by a quasiperiodic TBM, as well as to the quadratic rotor which is *not* quasiperiodic. We demonstrate that the Fibonacci decimation scheme is a very efficient method to compute fluctuations in the localization lengths irrespective of the nature of the aperiodicity of the TBM. Note that for nonquasiperiodic problems, Fibonacci decimation can be replaced by a more conventional one where every other site is decimated. Finally, we note that for quasiperiodic systems where the incommensurability is characterized by an arbitrary irrational number, a decimation scheme based on a Farey tree has been developed [10]. The fractal characteristics of such systems do not exhibit the self-similarity that underlies incommensurate systems with golden mean or other related quadratic irrationals. Apart from this difference, most of the results discussed below are valid for arbitrary irrationals.

After the nth decimation level, the nearest-neighbor TBM connecting the fluctuations at two neighboring Fibonacci sites is written as

$$f_n(m)\,\eta(m+F_{n+1}) = \eta(m+F_n) + e_n(m)\,\eta(m). \quad (14)$$

This equation describes a flow in Fibonacci space (labeled by the index n) where the original TBM [Eq. (13)] determines the initial conditions for the functions e_n and f_n, which we will refer to as the decimation functions. These functions can be determined using *exact* recursion relations [9]

$$e_{n+1}(i) = -\frac{Ae_n(i)}{1+Af_n(i)}, \quad (15)$$

$$f_{n+1}(i) = \frac{f_{n-1}(i+F_n)f_n(i+F_n)}{1+Af_n(i)}, \quad (16)$$

$$A = e_{n-1}(i+F_n) + f_{n-1}(i+F_n)e_n(i+F_n).$$

The derivation of these relations involves simple manipulations which exploit the additive property of the Fibonacci numbers [9,10]. These can now be iterated to machine precision as they do not depend on any parameter which could limit the precision. It turns out that for the localized phase where γ is always greater than zero, the decimation function f_n vanishes asymptotically and hence the resulting renormalization flow simplifies to

$$e_{n+1}(i) = -e_{n-1}(i+F_n)e_n(i). \quad (17)$$

In view of this further simplification, the above equation can be iterated up to 35 iterations, which corresponds to studying TBM of size up to 14 930 352.

Any fractal character in the fluctuations can be inferred by nontrivial asymptotic behavior of the functions e_n. In particular, the convergence of the renormalization flow either to a nontrivial limit cycle (which implies self-similarity) or a strange set is a clear indication of fractality.

It is interesting to note that the decimation function e_n also determines the localization length as $\gamma - \overline{\gamma} = \ln|e_n|/F_n$. When the $\overline{\gamma}$ is not known, the above equation determines it self-consistently to a very high precision.

In order to calculate the exponential line shape for a given quasienergy, we iterate the TBM [Eq. (8)]. Starting from the site at $+N$, we iterate the equation backwards and simultaneously iterate forwards from site $-N$. We then match these backward and forward iterates at $m=0$ by adjusting the phase factor ω, thereby determining the quasienergy. Note that in this method, the localization center is always at $m=0$.

An extremely accurate method to determine the quasienergies results from rewriting the TBM as a quasiperiodically driven map [11]. This is obtained by defining

$$x_m = u_{m-1}/u_m, \quad (18)$$

which transforms the TBM to

$$x_{m+1} = \frac{-1}{x_m + \lambda \tan\{[\omega - K(m)]/2\}}. \quad (19)$$

The localized phase of the TBM manifests itself as a strange nonchaotic attractor of this map, reflected in the expression for the Lyapunov exponent of the map $\mu = -2\gamma$ [11]. The negative sign is crucial as it implies that an attractor with $\mu < 0$ corresponds to diverging u_m with increasing m. Similarly, an attractor of the inverse map corresponds to diverging u_m with decreasing m. Thus, an exponentially localized function is obtained by starting from the intersection points of these two attractors and reversing the direction of iteration in each case. The quasienergies of the kicked rotor are used as tunable phase factors to ensure that *the intersection points of the attractor always occur* at $m=0$. This provides an extremely accurate method to compute the quasienergies. The resulting u_m is exponentially localized in both directions with the localization center m_0 always at zero. Note that a consequence for the results we show is that the lattice site label is *always relative to the localization center*.

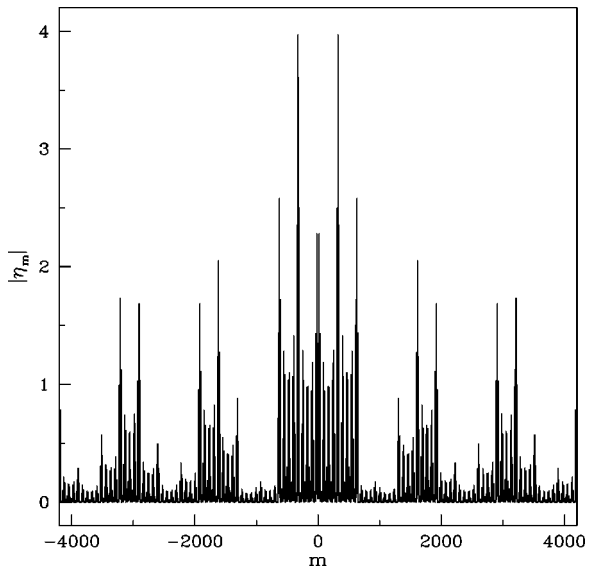

FIG. 1. Self-similar fluctuations in a linear rotor for $\omega = 0$. The fluctuations repeat themselves at every sixth Fibonacci site, that is, $F(6)$, $F(12)$, etc. This type of ''translational invariance'' in Fibonacci space is described by a period-6 limit cycle of the renormalization flow. Note that this behavior is independent of the kicking parameter k. In this and all other figures, the units are dimensionless.

As stated earlier, the primary difference between the linear and quadratic rotors lies in the character of the fluctuations. In both cases, the rotor wave function u_m, with exponentially decaying envelope, exhibits fractal fluctuations η_m which decay as a power law, $\eta_m \approx m^p$. The exponent p is related to the decimation function as $p(n) = \ln[|e_n|]/\ln(F_n)$. Asymptotically (in the limit of large decimation level), $e(n) \approx \eta(F_n)$, the exponent p is a measure of the fluctuations in the exponent γ as $p(n) = (\gamma_n - \overline{\gamma})(F_n)/\ln(F_n)$. Note that the measure $p(n)$ depends on the decimation level n. The behavior of p with kicking parameter k distinguishes the two rotor cases we consider.

Figure 1 shows the self-similar fluctuations η_m, for $\omega = 0$, in the case of the linear rotor. It should be noted that the fluctuations are described by a nontrivial period-6 limit cycle of the renormalization flow, that is, $\eta_{F_n} = \eta_{F_{n+6}}$. Further, the same period-6 was found for all values of k thereby establishing the fact that the fractal fluctuations are independent of k for $k > 0$. The multifractal nature of these fluctuations was also confirmed by the $f(\alpha)$ curve. For other values of

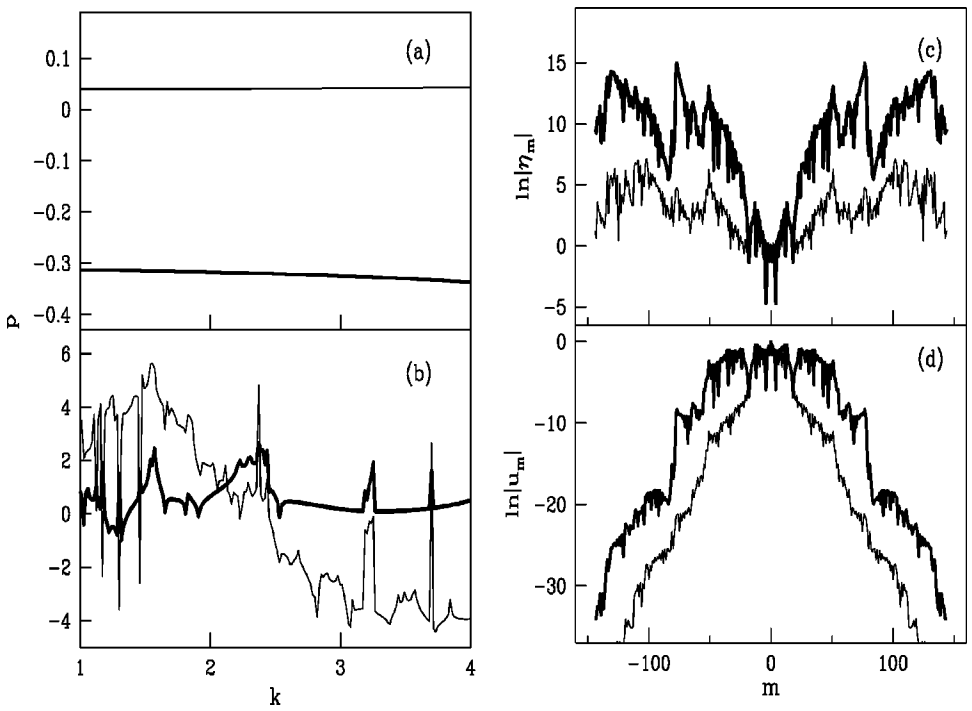

FIG. 2. The variation in the power law exponent $p(n)$ as a function of the kicking parameter k is shown for (a) the linear and (b) quadratic rotors at two different decimation levels. The darker and lighter curves, respectively, correspond to the 12th and 15th decimation level. (c) shows the fluctuations η_m versus m for the quadratic rotor at $k=3.252$ (darker curve) and at $k=2.9$ (lighter curve). Note that the larger value of k corresponds to a peak (spike) in (b) while the other does not. The jump in magnitude of the fluctuations is seen in the corresponding line shapes shown in (d), with larger fluctuations leading to ''shoulders'' seen in the line shape. These ''shoulders'' result in variations in localization length from the corresponding asymptotic values.

quasienergies, the fluctuations are not described by a limit cycle. Instead, the decimation functions e_n (for all quasienergies) converge on an invariant set with fractal measure, independent of k. For our purposes, it is more illustrative to focus on the impact of these features on the localized line shape. Given the relationships constructed earlier, this universality implies that *the convergence of the localization length* γ_n^{-1} to the asymptotic value $\overline{\gamma}^{-1}$ *is also independent of* k.

As seen from Fig. 2(a), the universality in the linear rotor is reflected in $p(n)$, which is independent of k at different decimation levels. In contrast to the linear rotor, the quadratic rotor shows fluctuations which depend strongly on k. As seen from Fig. 2(b), the power $p(n)$ exhibits many spikes as a function of the parameter k. These spikes are the result of local ''resonances'' in the fluctuations. The nature of these resonances is seen from Fig. 2(c) where η_m changes by several orders of magnitude within a few sites. The location in m and the magnitude of these ''jumps'' depend both on k and the quasienergy ω. Two values of k are shown in Fig. 2(c) with the dark curve ($k=3.252$) corresponding to a larger spike (for both n) in Fig. 2(b). Figure 2(d) shows that the resonances lead to ''shoulders'' in the exponential line shape, indicating local variation in the exponential envelope. It is worth noting that the quasienergies vary with k and are computed for each k using the matching condition described earlier.

The location of the resonance determines the impact of these local deviations. If the resonance occurs close to the localization center, then the deviations in γ from $\overline{\gamma}$ are clearly significant. However, if the resonance site is far from the localization center, then the exponential envelope diminishes the importance of the deviations. Figure 3 shows the line shapes associated with single quasienergy states for both

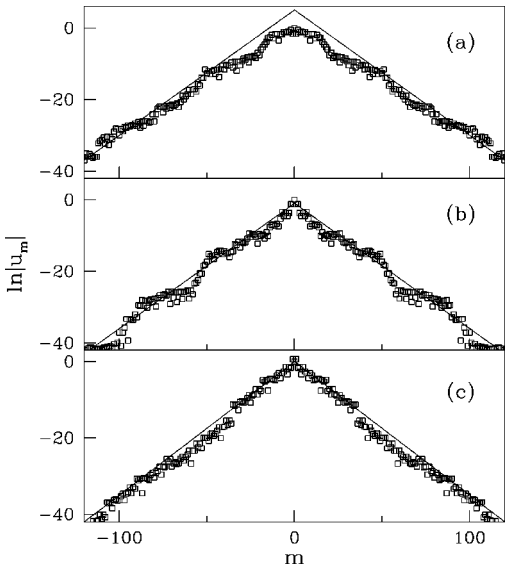

FIG. 3. Single localized quasienergy states (points) for the quadratic rotor (a) and (b) and the linear rotor (c). The parameter $k=2.8$. Note that (a) and (b) correspond to quasienergies 0.00 and 0.17, respectively. The linear rotor case is computed for $\omega=0$. The Lloyd model prediction for the localization length $\overline{\gamma}^{-1}$ is plotted in each case (solid line) to guide the eye.

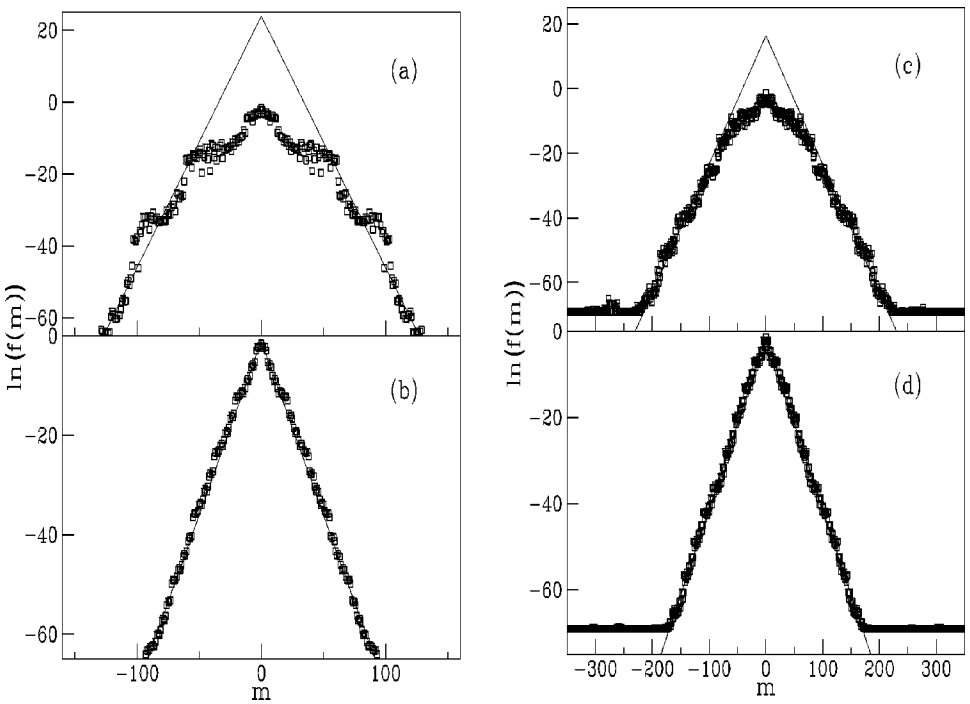

FIG. 4. Localized line shapes (points) starting from a plane-wave initial condition for linear [(b) and (d)] and quadratic [(a) and (c)] rotors. The first column considered $k=2.8$ while the second is for $k=5$. In all cases, the solid line indicates the Lloyd model result.

rotors. As seen from the linear rotor line shape in Fig. 3(c), the *absence of resonances* means that the Lloyd model estimate is a very good approximation to the actual calculated localization length, *all the way to the localization center*. This result was found to be true for all quasienergies and for all values of the kicking parameter k. However, for the quadratic rotor shown in Figs. 3(a) and 3(b), the Lloyd model estimate of γ^{-1} appears to be correct only in the tails of the localized line shape for most of the quasienergies. Deviations from the asymptotic $\overline{\gamma}^{-1}$ depend strongly on both the parameter k and the quasienergy, as seen by contrasting Fig. 3(a) and Fig. 3(b). For $\omega=0.17$, $\overline{\gamma}^{-1}$ is clearly a better fit for the associated quasienergy state than for the case of $\omega=0$.

Therefore, localization in the quadratic rotor starting from an initial wave packet composed of several quasienergy states should not be well described by the Lloyd model. To illustrate this, we consider the evolution of a plane wave (at $m=0$) under the repeated action of the single-step evolution operator U. The canonical method of fast Fourier transforms is used to get the localized line shape after a large number of kicks. The probability distribution $f(m)$ across lattice sites m is then constructed. As seen from Fig. 4, the linear rotor [(b) and (d)] coincides with the Lloyd model prediction all the way to the localization center. This is in stark contrast to the case of quadratic rotor in Figs. 4(a) and 4(c) where the deviations are strongest close to the localization center. It is also evident that the magnitude of these deviations depends on k. Exponential fits near the centers of the line shapes yield values of γ^{-1} which are clearly different from the asymptotic estimates given by $\overline{\gamma}^{-1}$.

The conditions under which the Lloyd model calculation [8] was made allow us to speculate on the possible reasons for both the resonances and the associated deviation in γ. The calculation of the estimate $\overline{\gamma}$ required the T_n to satisfy a specific distribution. However, dynamical phase correlations would lead to a violation of this requirement. This was verified both by constructing the return mapping for the on-site potentials and by directly plotting a histogram of on-site terms and contrasting with the required distribution. These were noted in earlier work as well [3,4] and are clearly different in the linear and quadratic cases.

We believe that the local resonances and fluctuations seen in the localization characteristics of the quadratic rotor are generic to pseudorandom systems. We have verified that TBM with bounded on-site potentials such as $\cos(2\pi\sigma m^{\nu})$ also exhibit characteristics similar to that of the quadratic rotor for $\nu>2$. $\nu=1$ constitutes a special case as the model reduces to the well-known quasiperiodic Harper equation [12], where the fractal localization character was also found to be independent of the coupling [9]. It should be noted that the Harper equation has been recently solved using the Bethe ansatz [13], implying some sort of ''integrability'' in the model. In view of this, we speculate that for the linear rotor, the k independence results from the integrable nature of the problem.

Ideally, in quadratic rotors, the possibility of correlations can be recognized from studying the classical dynamics resulting from the kicked rotor Hamiltonian. Specifically, in the context of quantum dynamics in mixed phase spaces, quantum phase correlations can be associated with the presence of invariant structures in the classical phase space. This relationship is of great current interest in the new context of quantum manifestations of classical anomalous transport [14,15]. Recent work suggests that there may be a relationship between large fluctuations in the localization length and the anomalous diffusion in the classical phase space

[14]. The line shapes also exhibit shoulders similar to the ones shown here. We propose to examine more closely the association of quantum phase correlations with structures in the associated classical phase space. However, as mentioned earlier, this is not possible in the special class of rotor studied here as the corresponding classical mapping is not well defined. In keeping with this general motivation, we are presently extending our work to models where this is not an issue.

The research of I.I.S. was supported by a grant from the National Science Foundation (Grant No. DMR 093296). The work of B.S. was supported by the National Science Foundation and a grant from the City University of New York PSC-CUNY Research Award Program.

[1] See, for example, the discussion in L.E. Reichl, *The Transition to Chaos In Conservative Classical Systems: Quantum Manifestations* (Springer-Verlag, New York, 1992).
[2] *Quantum Chaos: Between Order and Disorder : A Selection of Papers*, edited by G. Casati and B.V. Chirikov (Cambridge University Press, New York, 1995).
[3] S. Fishman, D.R. Grempel, and R.E. Prange, Phys. Rev. Lett. **49**, 509 (1982); Phys. Rev. A **29**, 1639 (1984).
[4] For a recent review, see S. Fishman, in *Quantum Dynamics of Simple Systems: The 44th Scottish Universities Summer School in Physics*, edited by G.L. Oppo, S. M. Barnett, E. Riis, and M. Wilkinson (Scottish Universities Summer School in Physics and Institute of Physics Pub., Bristol, 1996).
[5] F.M. Izrailev, Phys. Rep. **196**, 299 (1990).
[6] P.W. Anderson, Phys. Rev. **109**, 1492 (1958).
[7] P.A. Lee and T.V. Ramakrishnan, Rev. Mod. Phys. **57**, 287 (1985).
[8] P. Lloyd, J. Phys. C **2**, 1717 (1972).
[9] J.A. Ketoja and I.I. Satija, Phys. Rev. Lett. **75**, 2762 (1995); Phys. Lett. A **194**, 64 (1994).
[10] J.A. Ketoja and I.I. Satija, Physica A **219**, 212 (1995).
[11] J.A. Ketoja and I.I. Satija, Physica D **109**, 70 (1997).
[12] P.G. Harper, Proc. Phys. Soc. London, Sect. A **68**, 874 (1955).
[13] P.B. Wiegmann and A.V. Zabrodin, Phys. Rev. Lett. **72**, 1890 (1994).
[14] Bala Sundaram and G.M. Zaslavsky, Phy. Rev. E **59**, 7231 (1999).
[15] B.G. Klappauf, W.H. Oskay, D.A. Steck, and M.G. Raizen, Phys. Rev. Lett. **81**, 4045 (1998).